

## Research Article

Xiao-Hang Zou, Si-Wei Zhao, Ji-Guo Zhang, Hui-Liang Sun, Qing-Jiang Pan\*, Yuan-Ru Guo\*

# Preparation of ternary ZnO/Ag/cellulose and its enhanced photocatalytic degradation property on phenol and benzene in VOCs

<https://doi.org/10.1515/chem-2019-0088>

received January 23, 2019; accepted April 12, 2019.

**Abstract:** The ZnO/Ag/cellulose composite (ZAC) with excellent photocatalytic activity of degrading benzene and phenol in VOCs has been successfully synthesized. EDS, TEM, XPS and UV-vis analyses show that the ZAC is a ternary composite. It is composed of Ag, ZnO and cellulose, where the cellulose works as the substrate to anchor the other two components. The X-ray diffraction patterns find well-crystallized ZnO nanoparticles. Multiple PL peaks in the visible region measured for ZAC, imply rich defects on ZnO. It is observed that Ag nanoparticles are mainly attached on ZnO in the composite, which would raise the separation efficiency of photogenerated electrons and holes. Photocatalytic degradation shows that ZAC is able to decompose almost 100% phenol and 19% benzene in VOCs under UV light irradiation (6 W) which is almost no harm to human body. Due to the renewable cellulose, our ternary composite ZAC imparts low-cost, easily recycled and flexible merits, which might be applied in the indoor VOCs treatment.

**Keywords:** Biomaterial composite, ZnO, Degradation, Environmentally benign, VOCs.

## 1 Introduction

As major organic pollutants, volatile organic compounds (VOCs) cause great concern due to their adverse effects

on human health. According to previous studies, VOCs can induce cancer, respiratory diseases and other long term health risks, which are closely related to mortality and morbidity [1]. Especially to indoor air, the VOCs that escaped from adhesive in furniture or floors are harmful to human health. To solve this issue, many physical and chemical methods have been proposed and studied, such as biofilters, adsorption, catalytic oxidation and ozonation [2]. However, an effective, low-cost, nontoxic and non-secondary pollution method for indoor-air cleaning still remains challenging for scientists.

In the past decades, ZnO has been widely studied because of its great potential in nano-device research [3-5]. ZnO has a 3.37 eV band gap and large exciton binding energy, which enables it to possess good physical and chemical properties [6]. It is a promising material for fabricating photodetectors, light-emitting diodes, solar cells and photocatalysts [7-10]. Due to the characteristics of ZnO nanostructures, impurities or quantum dots like graphene can be added to enhance the photoelectric and photocatalytic properties [11]. In addition, noble metal nanoparticles have been incorporated with ZnO to form Schottky heterojunctions. Because the surface plasmon resonance of precious metals matches ZnO nanoparticles, the photoelectric properties are greatly improved. In Ag/ZnO composites, Ag can be used as an electron acceptor, which can effectively capture electrons, promote the separation of light-generated electrons and holes, and, effectively, improve the photocatalytic performance of Ag/ZnO [12,13]. Due to this advantage, many researchers have investigated Ag/ZnO for its potential applications as an antibacterial, water-purifying reagent or ultraviolet photodetector [14-16]. However, controlling the synthesis of Ag/ZnO with the desired performance is still a problematic problem to solve [17-23].

Cellulose, as a regenerated bioresource, has been widely studied in recent years. As assemblies of microfibers with full of hydroxyl groups, it is easy to combine with other materials via hydrogen bonding. Although normal cellulose does not process functional photo/

\*Corresponding authors: Qing-Jiang Pan, Key Laboratory of Functional Inorganic Material Chemistry (Ministry of Education), School of Chemistry and Materials Science, Heilongjiang University, Harbin 150080, China, E-mail: panqjtc@163.com; Yuan-Ru Guo, Key Laboratory of Bio-based Material Science & Technology (Ministry of Education), College of Material Science and Engineering, Northeast Forestry University, Harbin 150040, China, E-mail: guoyrnefu@163.com  
Xiao-Hang Zou, Si-Wei Zhao, Ji-Guo Zhang, Hui-Liang Sun, Key Laboratory of Bio-based Material Science & Technology (Ministry of Education), College of Material Science and Engineering, Northeast Forestry University, Harbin 150040, China

electrochemical property, it has many other advantages, such as: cheapness, natural reproduction, easy recovery and easy-processing. These advantages make cellulose a good substrate candidate for preparing cellulose-based composites. Thus, cellulose composite has attracted extensive attention of researchers and many related works have been reported [24-29].

In this work, we used ultrasonic-assisted hydrothermal method to synthesize the ZnO/Ag/cellulose (ZAC) composite. The results indicate that the ZAC possesses the enhanced photocatalytic activity compared with ZnO/cellulose [30]. The photocatalytic property of degrading benzene, phenol and their derivatives were fully studied. It is shown that our ZAC composite may be a promising material in cleaning the indoor air.

## 2 Experimental

### 2.1 Materials

The source materials, such as, sodium hydroxide (NaOH) and zinc acetate dehydrate ( $\text{Zn}(\text{CH}_3\text{COOH})_2 \cdot 2\text{H}_2\text{O}$ ) were bought from Tianjin Yongda Chemical Reagent Company Limited and Tianjin Kemiou Chemical Reagent Company Limited, respectively. Coniferous filter paper was used as source of cellulose, which was bought from Hangzhou Special Paper Company Limited.  $\text{AgNO}_3$ ,  $\text{NaBH}_4$  and polyvinyl pyrrolidone (PVP) were bought from Tianjin Tiangan Chemical Technology Development co., LTD, Tianjin Kemiou Chemical Reagent Company Limited and Shanghai Qiangshun Chemical Reagent Company Limited, respectively.

### 2.2 Preparation of cellulose@ZnO

Cellulose@ZnO composite was prepared by the hydrothermal method used in previous research [30]. 3.0 g zinc acetate and 1.0 g cellulose were dissolved in 25 mL distilled water. After stirred vigorously for 1 hour, the pH value of the solution was adjusted to 8~12 using 1 mol·L<sup>-1</sup> sodium hydroxide solution. The white cellulose suspension was obtained after 1h stirring. Then, the cellulose suspension was put into a 100 mL steel autoclave and heated at 100 °C for ten hours. The white turbid liquid was filtered after being cooled to room temperature, and the white products were collected. ZnO/cellulose composite paper was obtained after being dried at 80 °C.

### 2.3 Preparation of ZnO/Ag/cellulose

0.08 g of PVP was dissolved in 60 mL distilled water and then added 8 mL of 6 mmol·L<sup>-1</sup>  $\text{AgNO}_3$ . After stirring for 20 min, 60 mL 0.008 mol·L<sup>-1</sup> of  $\text{NaBH}_4$  solution was added into mixed solution slowly. After 2 hours of stirring, the yellow Ag solution was obtained.

0.1 g of ZnO/cellulose was added into 15 mL of Ag solution under nitrogen protection for 5 min and stirred 30 min later. After 20 min of ultrasonic concussion treatment, the mixed solution was heated in a water bath at 60 °C for 30 min. The final products were obtained after filtration, drying and washing with deionized water. According to the pH value during preparation of ZnO/cellulose, the ternary composites of ZnO/Ag/cellulose were named as ZAC-8, ZAC-9, ZAC-10 and ZAC-12, respectively.

### 2.4 Characterization

The crystallinity and purity of the ZnO was characterized by X-ray diffraction (XRD; Rigaku D/Max-RC, Tokyo, Japan). The data were recorded using Cu K $\alpha$  radiation (wavelength of 1.5418 Å) and working at 40 mA and 40 kV with a scan rate of 4°/min. The morphology of the ZnO was characterized by field emission scanning electron microscope (FE-SEM, S-4800 Hitachi, Ltd. Chiyodaku Japan). And the high-resolution transmission electron microscopy (HRTEM; JEM-2100, JEOL, Japan) was, also, performed to study the construction of components in ZAC. Photoluminescence study was recorded on a Perkin Elmer fluorescence spectrophotometer (U.K.) at room temperature. The excitation wavelength is 355 nm, the Ex slit was 10.0 nm and the scan speed was 1200 nm/min. The elemental analysis and the binding energy were studied by XPS (K-Alpha, Thermofisher Scientific Company, US).

The photocatalytic activity of prepared ZAC was tested by degrading methylene blue (MB). In a typical experiment, 0.05 g ZAC was put into 80 mL MB solution (20 mg·L<sup>-1</sup>) to form a suspension. Stirring handling was kept in the whole process unless otherwise noted. Then, the suspension was retained in the dark for 30 min to achieve the absorption-desorption equilibrium. Later on, the suspension was exposed to the UV irradiation (YZ-GHX-A, 300W, Shanghai Jingmi Instrument Co. Ltd.) under ambient conditions. In order to evaluate the degradation efficiency, the suspension was sampled and analyzed every 30 min. The degradation was measured by recording variations at the maximum absorption around  $\lambda=664$  nm using UV-vis spectrophotometer at a definite

time interval (TU-1901, Beijing Purkinje Genral Instrument Co. LTD, China).

The photocatalytic properties were also explored by phenol, benzene and their derivatives. A *larix gmelinii* wood sample (150×100×20 mm) was brushed with urea-formaldehyde resin adhesive (UF). For the photocatalytic experiment, the wood sample with UF was put into a sealed vessel with 0.1 g ZAC, and then irradiated by UV light (245nm, 6 W). After 24 hours irradiation, the air sample was analyzed by DSQII GC-MS (USA, Thermo Co. LTD). A control experiment was also carried out without ZAC and UV irradiation.

Ethical approval: The conducted research is not related to either human or animal use.

### 3 Results and discussion

#### 3.1 XRD analysis

X-ray diffraction analysis has been used to identify the crystal structure of ZAC. The XRD plots of cellulose, sintered ZnO and ZAC-12 are shown in Figure 1. As we can see from Figure 1, the diffraction peaks at 15.04°, 16.16° and 22.87° are identified to (101), (001) and (002) lattice planes of cellulose I. Diffraction peaks at 31.94°, 34.50°, 36.37°, 47.67°, 56.62°, 62.90° and 67.94° belong to the (100), (002), (101), (102), (110), (103), and (112) crystalline planes of ZnO. Those peaks match perfectly to the hexagonal wurtzite crystal structure of ZnO (JCPDS No. 36-1451) which indicates the existence of ZnO in composite. Compared to sintered ZnO and cellulose, only diffraction peaks of ZnO and cellulose are observed in the composite, which gives the evidence that there is no other impurity in the ZnO/Ag/cellulose composite. Due to the trace content of Ag in composite, there is no diffraction peaks of Ag could be found in the XRD plot.

#### 3.2 FE-SEM, TEM and EDS analysis

SEM has been used to characterize the morphology of ZAC composite. The morphology of all ZAC composites are shown as the cellulose fiber-assemblies, to which ZnO particles are attached (Figure 2). The contents and the morphology of ZnO particles on cellulose are dependent on the pH of the synthesizing solution. In low pH conditions, small ZnO particles are found on the surface of cellulose (Figure 2a-c); increase the pH to 12, ZnO microparticles about 300 nm length and 50 nm width

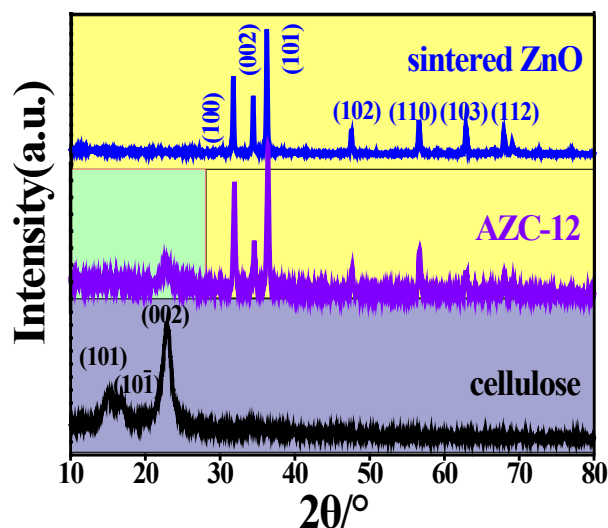


Figure 1: XRD plots of cellulose, sintered ZnO and ZAC-12.

are observed (Figure 2d). According to a previous study, ZnO nanoparticles with certain sizes are easily to self-assemble with cellulose [30]. However, in this study, we didn't find the same size ZnO nanoparticles on prepared cellulose composite. This was caused by the ultrasonic concussion treatment during the process of introducing Ag into the composite. Since the interaction between the ZnO and cellulose is hydrogen bonding, it is possible that ZnO would fall off from the cellulose during ultrasonic concussion.

EDS has also been applied to analyze the components of composite. According to Figure 2f, both ZnO and Ag are found in the cellulose composite, which indicated that ternary composite of ZAC have been successfully fabricated by our method.

To fully understand the microstructure of composite, TEM images of ZAC-12 is shown in Figure 3. From Figure 3a and b, we can see the Ag nanoparticles about 5 nm adhere on ZnO microparticles. The crystal inter planar spacing is 0.23 nm (Figure 3c and d), which was attributed to the (111) planar spacing of Ag nanoparticles [31]. 0.16 nm is attributed to the (002) planar spacing of ZnO [32]. The TEM images also give the evidence that Ag nanoparticles can bind with ZnO.

#### 3.3 XPS analysis

Figure 4 are the XPS spectra of ZAC-12. From Figure 4a, one can see the spectrum of C 1s region. C 1s shows three peaks centering at 284.2 eV, 285.8 eV and 287.4 eV. The peak at

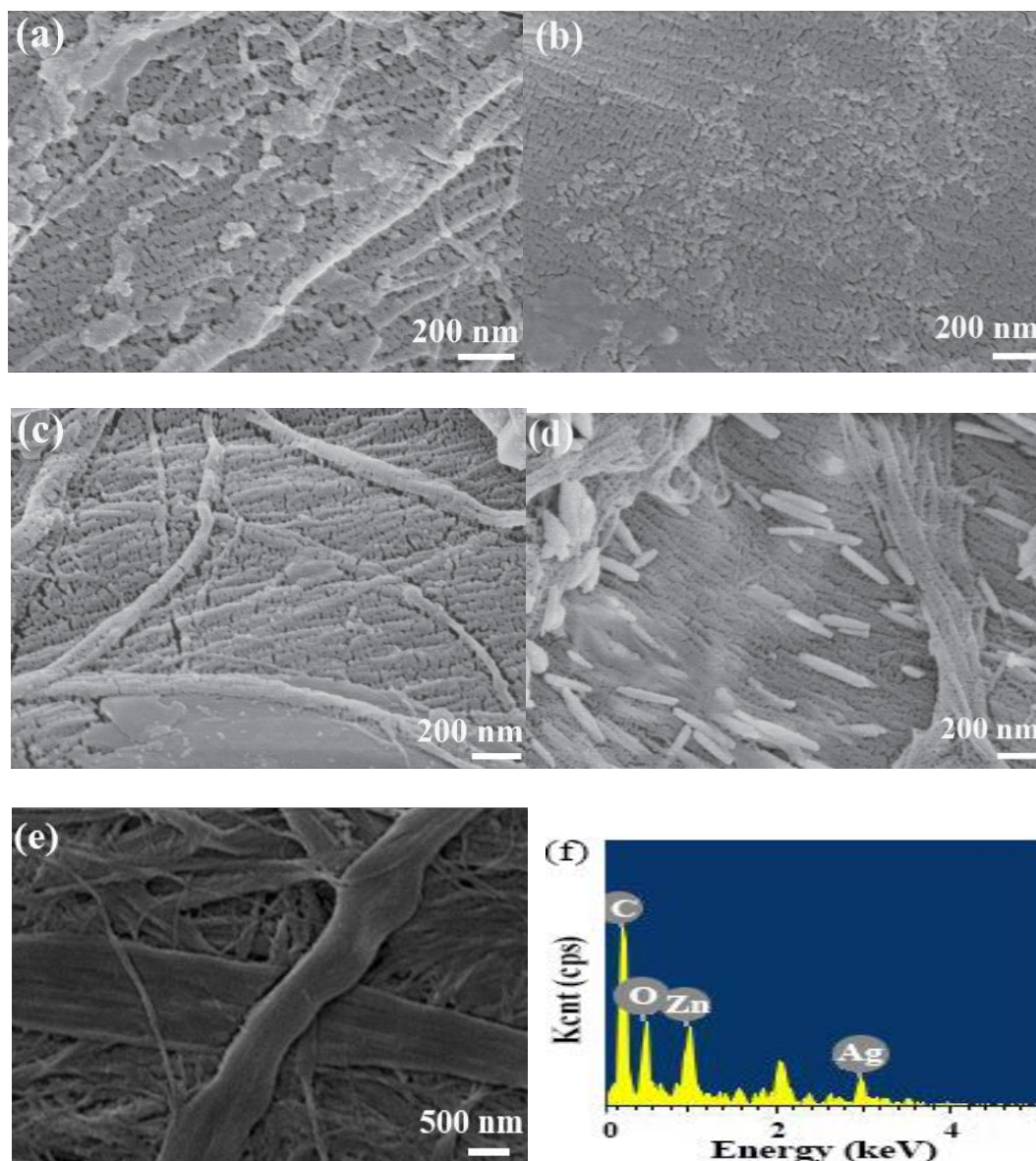


Figure 2: SEM images of ZAC composite samples (a) ZAC-8, (b) ZAC-9, (c) ZAC-10, (d) ZAC-12, (e) pure cellulose and (f) EDS of ZAC-12.

284.2 eV was corresponding to the carbon of alkyl (C–C/C–H, absorbed) in cellulose [33]. And the peak at 285.8 eV corresponds to the hydroxyl groups (C–OH) in cellulose [34,35]. And the peak at 287.4 eV can be attributed to C–O–C of cellulose [35]. The high resolution XPS spectrum for the O 1s region is shown in Figure 4b. The peak attributed to the O atom of ZnO is observed at 530.3 eV [36]. And the peak at 532.0 eV is the oxygen of hydroxyl groups (C–OH) in cellulose [37,38]. The binding energies at 368.0 eV and 374.1 eV are corresponding to  $\text{Ag}3d_{5/2}$  and  $\text{Ag}3d_{3/2}$  in Figure 4c [39,40]. The binding energies of Zn  $2p_{3/2}$  and Zn  $2p_{1/2}$  is shown in Figure 4d, which determined to be 1021.5 eV

and 1044.5 eV, and the peak separation distance between them was 23.0 eV [41]. The XPS gives the evidence that ZAC composite has been successfully prepared by our method.

### 3.4 Photocatalytic activity analysis

The photocatalytic activity of ZAC have been evaluated by both MB in solution and VOCs in air. MB degradation results are shown in Figure 5. After 2.5 h, the degradation rates are more than 95% by ZAC. And ZAC-12 has the highest degradation efficiency of 99.5%, which is much higher



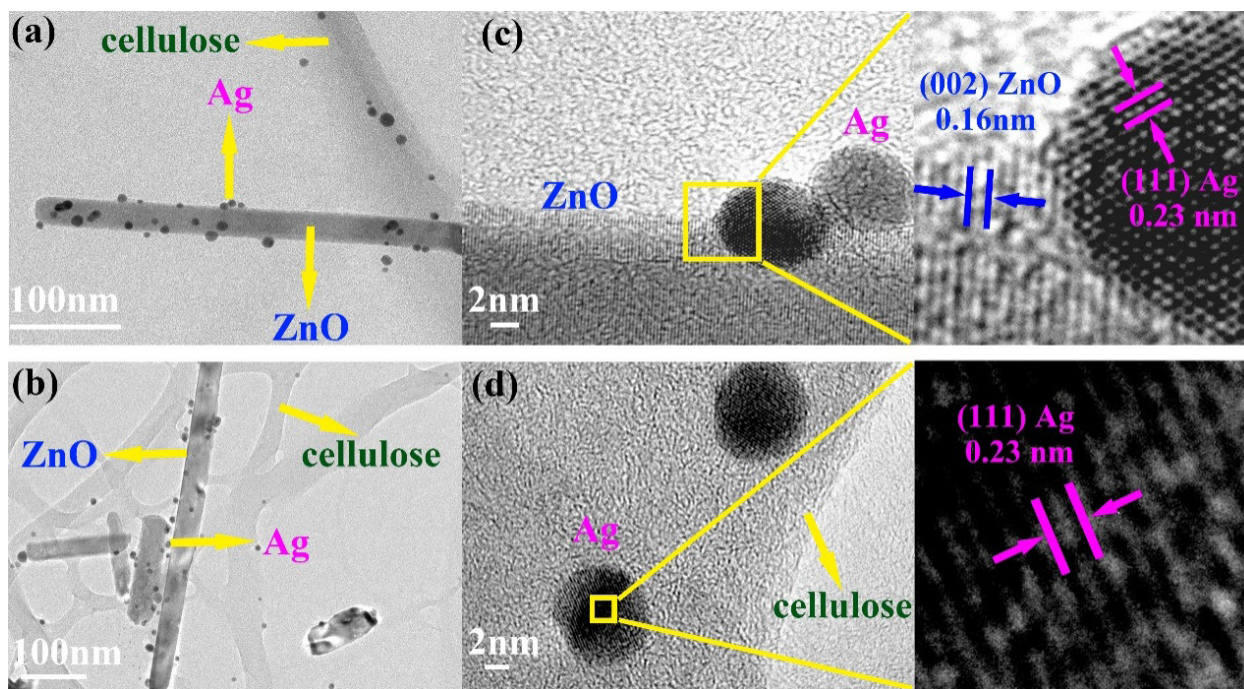


Figure 3: TEM images of ZAC-12 (a and b), and high-resolution transmission electron microscopy (HRTEM) images (c and d).

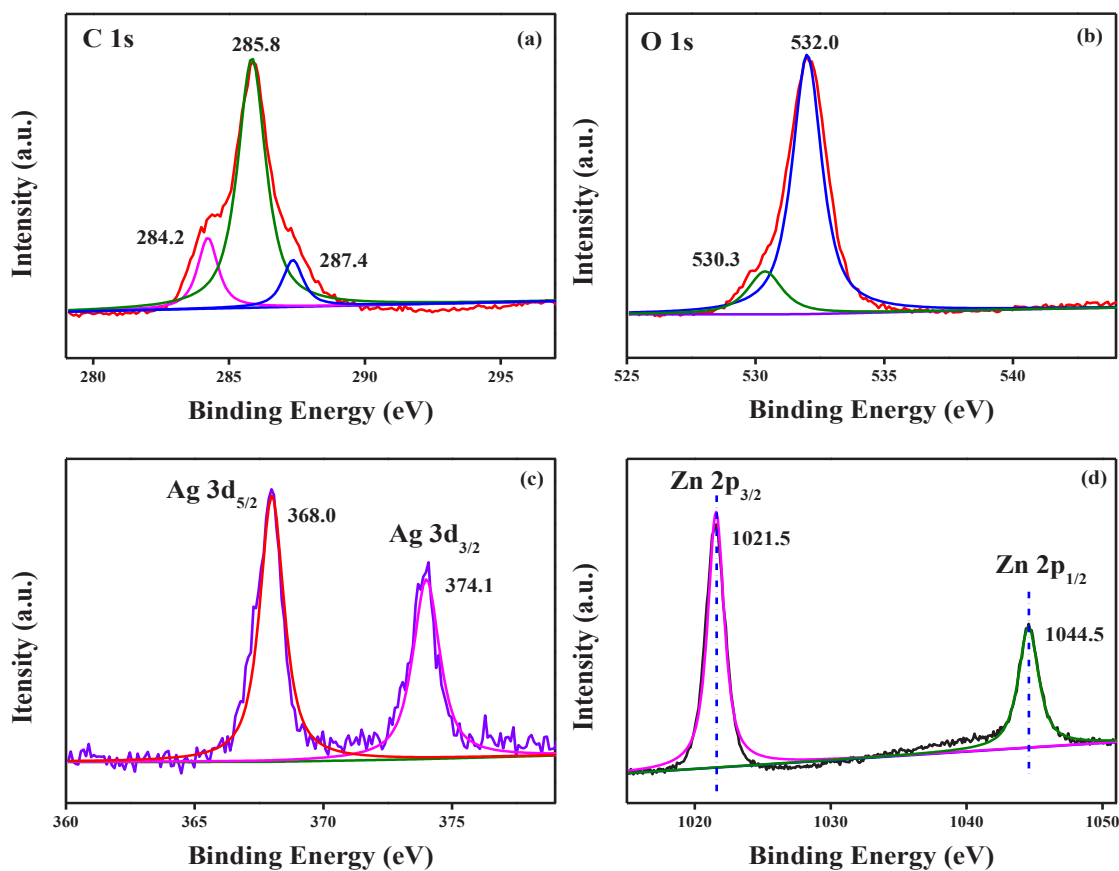
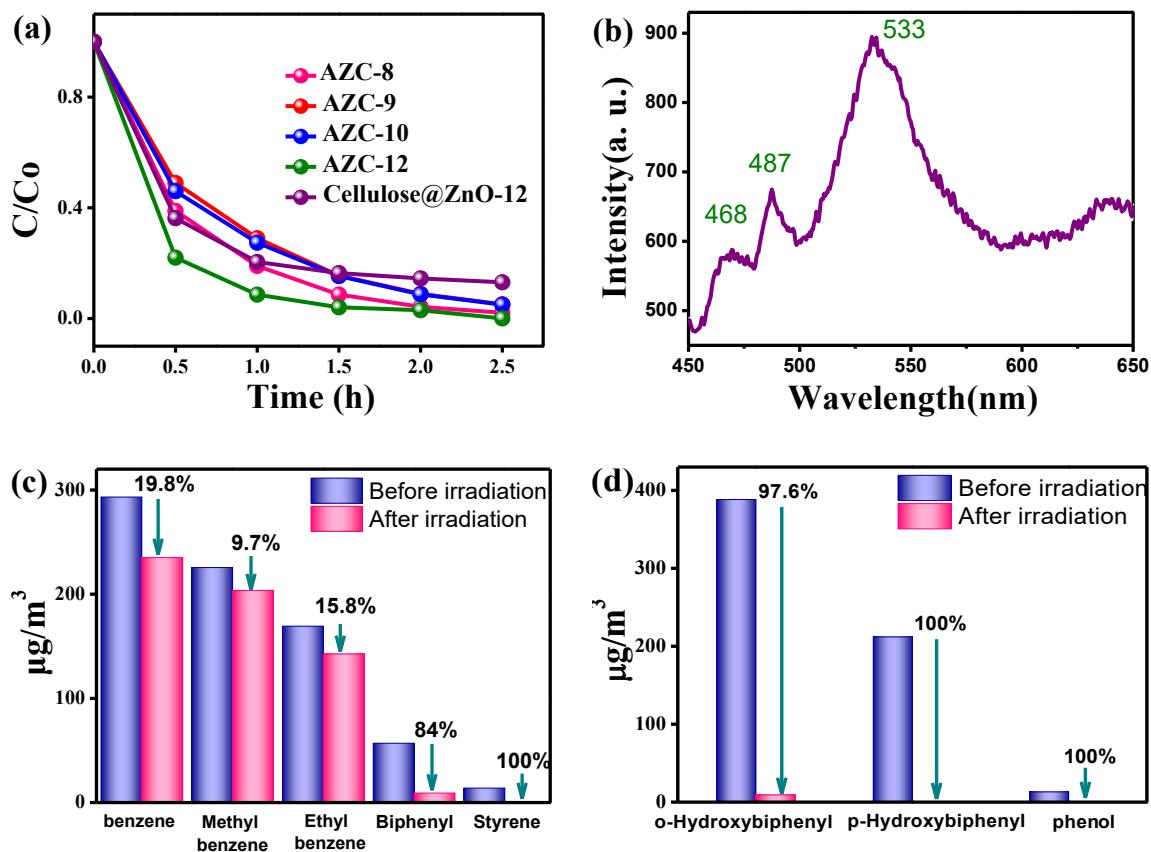


Figure 4: XPS of ZAC-12, C1s (a), O1s (b), Ag 3d (c) and Zn 2p (d).



**Figure 5:** Photocatalytic activity of ZAC composite evaluated by MB (a), PL spectrum of ZAC-12 (b), degradation of benzene, phenol and derivatives by ZAC (c and d).

than that of ZnO/cellulose (86.91%). This result indicates that ZAC composite possesses better photocatalytic activity after combination with Ag. Since Ag nanoparticles coated on the surface of ZnO, it would prefer to separate the electron and holes of ZnO, thus enhance the catalytic of ZAC. At the same time, photoluminescence (PL, Figure 5b) of ZAC-12 analysis show that there are three peaks in the visible region located at 468, 487 and 533 nm, which indicates that ZAC-12 has many defects. These defects would be beneficial to improve the photocatalytic property of ZAC-12 as well.

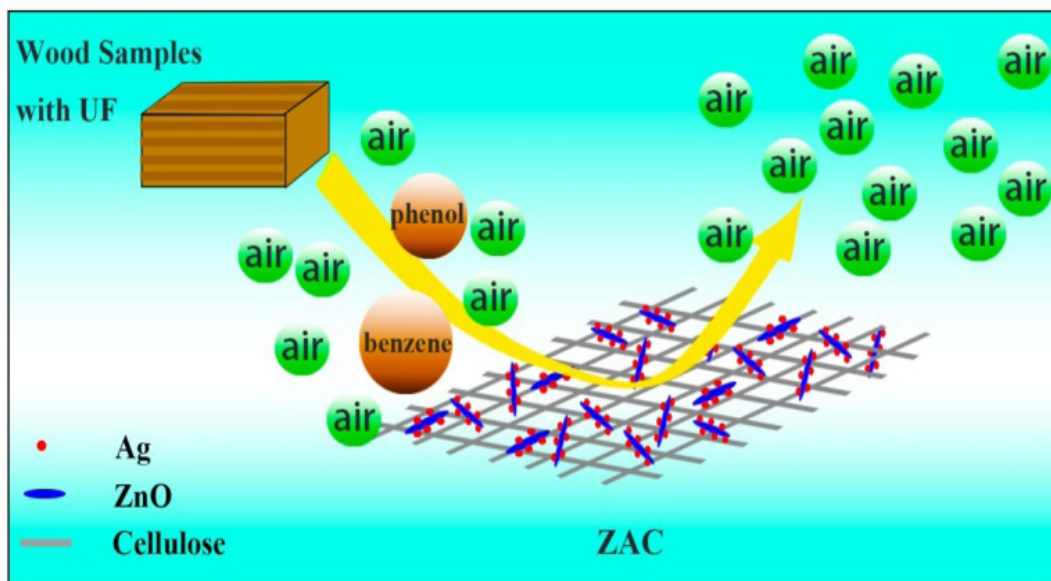
To understand the process, we further analyzed the photocatalytic reaction of ZAC with the first order kinetic equation  $\ln(C_0/C) = Kt$ . The fitting analysis shows that the photocatalytic reaction is the first-order kinetic reaction ( $R > 0.99$ ). The rate constant  $K$  of ZAC-8, ZAC-9, ZAC-10 and ZAC-12 is 1.53, 1.176, 1.17 and 2.56  $\text{h}^{-1}$ , respectively. ZAC-12 has the largest  $K$  value, which indicates that ZAC-12 has the best photocatalytic performance.

According to its good photocatalytic property on MB, the degradation on benzene and phenol and their

derivatives, which were volatilized by wood furniture, have been carried in a sealed environment. At the same time, a blank experiment was carried out as reference without using ZAC and irradiation. The results are shown in Figure 5c. From the Figure 5c, we can see that ZAC shows very good photocatalytic property on degradation of benzene and its derivatives. It can degrade styrene totally (100% degradation efficiency), and the degradation efficiency of benzene is also achieved to 19.7% in 24 hours. As to methyl benzene, ethyl benzene and biphenyl, the degradation efficiency is a little bit lower, which range from 8.4~15.8%.

And at the same time, ZAC shows excellent property on degradation of phenol compounds, as can be seen in Figure 5d. This result shows ZAC can degraded almost 100% of phenol, p-hydroxybiphenyl and o-hydroxybiphenyl. Especially to o-hydroxybiphenyl, which has high concentration of 359  $\mu\text{g}/\text{m}^3$  in the blank experiment, is degraded by efficiency of 97.1%.

To achieve such good property, we deduce that the ternary components in ZAC has a synergistic effect, as seen in scheme 1. Cellulose plays an important role.



**Scheme 1:** Photocatalytically degrading phenol and benzene by ZAC.

First, cellulose works as a substrate, which would guide the formation of ZnO on one hand, and endow ZAC the easy-shaping character. At the same time, it can adsorb the benzene or phenol and make them enrich around ZnO; on the other hand; ZnO is catalyst which property was enhanced by Ag nanoparticles. It is known that Schottky barriers at metal-semiconductor interface can improve the separation efficiency of electrons and holes [42-45]. The good photocatalytic performance of ZAC may be attributed to the formed Schottky barriers between the Ag NPs and ZnO in the composite. Under the UV irradiation, ZnO produces electron-hole pairs, and the Schottky barriers of ZnO/Ag inhibit the generated electron-hole recombination. With long lifetime of these separated electrons and holes, more reactive oxidative species can be generated. Consequently, more organic compounds would be degraded by reactive oxidative species.

Synergistic effects of cellulose, ZnO and Ag make our ZAC be a good candidate for further indoor air treatment.

samples. Its degradation rate for MB reaches 99.51%. The decomposition on phenol and benzene and their derivatives in VOCs were also investigated. It is shown that ZAC can degrade almost 100% phenol; even to difficultly decomposed benzene, it also exhibits good photocatalytic activity, around 19.8% degradation efficiency. The synergetic effect to enhance photocatalytic performance was endowed by the three components in the ZAC. Cellulose works as a substrate and adsorbent; ZnO /Ag together increases light-harvesting efficiency; and Ag NPs adhered on the ZnO surface raise separation efficiency of light-generated holes and electrons. Due to its easily-shaped, recycled merits and good catalytic properties, ZAC would be a good candidate for indoor air purification.

**Acknowledgments:** This work is supported by the Fundamental Research Funds for the Central Universities (2572018BB09) and Natural Science Foundation of Heilongjiang (C2018006).

**Conflict of interest:** Authors declare no conflict of interest.

## 4 Conclusions

The ZAC composite was successfully prepared by hydrothermal synthesis and ultrasonic method. According to TEM, EDS, XPS and UV-Vis spectroscopic characterizations, Ag NPs with 5 nm are mainly anchoring on the surface of ZnO. Specifically, ZAC-12 possesses the best photocatalytic activity among all ZAC composite

## Reference

- [1] Wu H., Yan H., Quan Y., Zhao H., Jiang N., Yin C., Recent progress and perspectives in biotrickling filters for VOCs and odorous gases treatment, *J. Environ. Manage.*, 2018, 222, 409-419.

- [2] Han M.F., Wang C., Fu Y., Treatment of hydrophobic volatile organic compounds using two-liquid phase biofilters, *Sci. Total Environ.*, 2018, 640, 1447-1454.
- [3] Khan N., Kumar A., Khan A., Wahab R., Khan S.T., Ahmad J., et al., Effect of praseodymium on the characteristics of nano-ZnO towards organophosphate as a nano-electrochemical device, *J. Nanoelectron. Optoe.*, 2016, 11, 6-11.
- [4] Ashok C.H., Rao K.V., ZnO/TiO<sub>2</sub> nanocomposite rods synthesized by microwave-assisted method for humidity sensor application, *Superlattice. Microst.*, 2014, 76, 46-54.
- [5] Seo Y.K., Kumar S., Kim G.H., Photoconductivity characteristics of ZnO nanoparticles assembled in nanogap electrodes for portable photodetector applications, *Physica E.*, 2010, 42, 1163-1166.
- [6] Bibi S., Shah A., Mahmood A., Ali Z., Raza Q., Aziz U., et al., Synthesis and characterization of binary ZnO-SnO<sub>2</sub> (ZTO) thin films by e-beam evaporation technique, *Appl. Phys. A-Mater.*, 2018, 124, 327.
- [7] Dong M., Wang Y., Li Z., Weng Z., Yu N., Simple fabrication of homogeneous ZnO core/shell nanorod arrays for ultraviolet photodetectors, *J. Nanosci. Nanotechnol.*, 2018, 18, 5686-5691.
- [8] Abdelfatah M., Ismail W., El-Shaer A., Low cost inorganic white light emitting diode based on submicron ZnO rod arrays and electrodeposited Cu<sub>2</sub>O thin film, *Mat. Sci. Semicon. Proc.*, 2018, 81, 44-47.
- [9] Huang Y.J., Chen H.C., Lin H.K., Wei K.H., Doping ZnO electron transport layers with MoS<sub>2</sub> nanosheets enhances the efficiency of polymer solar cells, *ACS Appl. Mater. Inter.*, 2018, 10, 20196-20204.
- [10] Zhao S.W., Zuo H.F., Guo Y.R., Pan Q.J., Carbon-doped ZnO aided by carboxymethyl cellulose: Fabrication, photoluminescence and photocatalytic applications, *J. Alloy. Compd.*, 2017, 695, 1029-1037.
- [11] Yao C., Xie A., Shen Y., Zhu W., Zhu J., Graphene oxide used as a surfactant to induce the flower-like ZnO microstructures: growth mechanism and enhanced photocatalytic properties, *Cryst. Res. Technol.*, 2014, 49, 982-989.
- [12] Xin Z., Li L., Zhang X., Zhang W., Microwave-assisted hydrothermal synthesis of chrysanthemum-like Ag/ZnO prismatic nanorods and their photocatalytic properties with multiple modes for dye degradation and hydrogen production, *Rsc Adv.*, 2018, 8, 6027-6038.
- [13] Ali A., Gul A., Ambreen S., Phull A.R., Zia M., Effective photocatalysis of direct dyes under sunlight by silver, iron, and zinc nanoparticles doped on cotton, *J. Environ. Chem. Eng.*, 2018, 6, 5915-5919.
- [14] Ali A., Pan M., Tilly T.B., Zia M., Wu C.Y., Performance of silver, zinc, and iron nanoparticles-doped cotton filters against airborne *E. coli* to minimize bioaerosol exposure, *Air Qual. Atmos. Hlth.*, 2018, 11, 1233-1242.
- [15] Liu Y., Zhang Q., Xu M., Yuan H., Chen Y., Zhang J., et al., Novel and efficient synthesis of Ag-ZnO nanoparticles for the sunlight-induced photocatalytic degradation, *Appl. Surf. Sci.*, 2019, 476, 632-640.
- [16] Khurshid F., Jeyavelan M., Hudson M.S.L., Nagarajan S., Ag-doped ZnO nanorods embedded reduced graphene oxide nanocomposite for photo-electrochemical applications, *Roy. Soc. Open Sci.*, 2019, 6, 181764.
- [17] Pelgrift R.Y., Friedman A.J., Nanotechnology as a therapeutic tool to combat microbial resistance, *Adv. Drug Deliver. Rev.*, 2013, 65, 1803-1815.
- [18] Alkaladi A., Abdelazim A., Afifi M., Antidiabetic activity of zinc oxide and silver nanoparticles on streptozotocin-induced diabetic rats, *Int. J. Mol. Sci.*, 2014, 15, 2015-2023.
- [19] Shanker K., Naradala J., Mohan G.K., Kumar G.S., Pravalika P.L., A sub-acute oral toxicity analysis and comparative in vivo anti-diabetic activity of zinc oxide, cerium oxide, silver nanoparticles, and *Momordica charantia* in streptozotocin-induced diabetic Wistar rats, *Rsc Adv.*, 2017, 7, 37158-37167.
- [20] Thongrom B., Amornpitoksuk P., Suwanboon S., Baltrusaitis J., Photocatalytic degradation of dye by Ag/ZnO prepared by reduction of Tollen's reagent and the ecotoxicity of degraded products, *Korean. J. Chem. Eng.*, 2014, 31, 587-592.
- [21] Singh S., Jit S., Park S.H., Characterization of Ag/ZnO nanorod Schottky diode-based low-voltage ultraviolet photodetector, *Nano*, 2017, 12, 1750063.
- [22] Mirershad F., Jafari A., Janati E., Roohi E., Sarabi M., Ag/ZnO Nano-composites as Novel Antibacterial Agent Against Strain of MRSA, *J. Pure Appl. Microbiol.*, 2013, 7, 947-956.
- [23] Sharma S.K., Ghodake G.S., Kim D.Y., Kim D.Y., Thakur O.P., Synthesis and characterization of hybrid Ag-ZnO nanocomposite for the application of sensor selectivity, *Curr. Appl. Phys.*, 2018, 18, 377-383.
- [24] Bai Q., Xiong Q., Li C., Shen Y., Uyama H., Hierarchical porous carbons from a sodium alginate/bacterial cellulose composite for high-performance supercapacitor electrodes, *Appl. Surf. Sci.*, 2018, 455, 795-807.
- [25] Li T.F., Wang X.Q., Jiao J., Liu J.Z., Zhang H.X., Niu L.L., et al., Catalytic transesterification of *Pistacia chinensis* seed oil using HPW immobilized on magnetic composite graphene oxide/cellulose microspheres, *Renew. Energ.*, 2018, 127, 1017-1025.
- [26] Yan Y., Chen T., Zou Y., Wang Y., Biotemplated synthesis of Au loaded Sn-doped TiO<sub>2</sub> hierarchical nanorods using nanocrystalline cellulose and their applications in photocatalysis, *J. Mater. Res.*, 2016, 31, 1383-1392.
- [27] Chen Y., Xu W., Liu W., Zeng G., Responsiveness, swelling, and mechanical properties of PNIPAA nanocomposite hydrogels reinforced by nanocellulose, *J. Mater. Res.*, 2015, 30, 1797-1807.
- [28] Wang D., Huang Y., Ma Y., Liu P., Liu C., Zhang Y., Research on highly sensitive humidity sensor based on Tr-MWCNT/HEC composite films, *J. Mater. Res.*, 2014, 29, 2845-2853.
- [29] Ali A., Gul A., Mannan A., Zia M., Efficient metal adsorption and microbial reduction from Rawal Lake wastewater using metal nanoparticle coated cotton, *Sci. Total Environ.*, 2018, 639, 26-39.
- [30] Zhao S.W., Zheng M., Zou X.H., Guo Y., Pan Q.J., Self-assembly of hierarchically structured cellulose@ZnO composite in solid-liquid homogeneous phase: synthesis, DFT calculations, and enhanced antibacterial activities, *Acs Sustain. Chem. Eng.*, 2017, 5, 6585-6596.
- [31] Kadam A.N., Bhopate D.P., Kondalkar V.V., Majhi S.M., Bathula C.D., Tran A.V., et al., Facile synthesis of Ag-ZnO core-shell nanostructures with enhanced photocatalytic activity, *J. Ind. Eng. Chem.*, 2018, 61, 78-86.
- [32] Singh S.K., Singhal R., Thermal-induced SPR tuning of Ag-ZnO nanocomposite thin film for plasmonic applications, *Appl. Surf. Sci.*, 2018, 439, 919-926.



- [33] Xing Z., Chen Y., Liu C., Yang J., Xu J., Situ Y., et al., Synthesis of core-shell ZnO/oxygen doped g-C<sub>3</sub>N<sub>4</sub> visible light driven photocatalyst via hydrothermal method, *J. Alloy. Compd.*, 2017, 708, 853-861.
- [34] Fu F.Y., Li L.Y., Liu L.J., Cai J., Zhang Y.P., Zhou J.P., et al., Construction of cellulose based ZnO nanocomposite films with antibacterial properties through one-step coagulation, *ACS Appl. Mater. Inter.*, 2015, 7, 2597-2606.
- [35] Boulos L., Foruzanmehr M.R., Tagnit-Hamou A., Elkoun S., Robert M., Wetting analysis and surface characterization of flax fibers modified with zirconia by sol-gel method, *Surf. Coat. Tech.*, 2017, 313, 407-416.
- [36] Abdel-Wahab M.S., Jilani A., Yahia I.S., Al-Ghamdi A.A., Enhanced the photocatalytic activity of Ni-doped ZnO thin films: Morphological, optical and XPS analysis, *Superlattice. Microst.*, 2016, 94, 108-118.
- [37] Le S., Jiang T., Li Y., Zhao Q., Li Y., Fang W., et al., Highly efficient visible-light-driven mesoporous graphitic carbon nitride/ZnO nanocomposite photocatalysts, *Appl. Catal. B-Environ.*, 2017, 200, 601-610.
- [38] Fu F., Gu J., Xu X., Xiong Q., Zhang Y., Liu X., et al., Interfacial assembly of ZnO-cellulose nanocomposite films via a solution process: a one-step biomimetic approach and excellent photocatalytic properties, *Cellulose*, 2017, 24, 147-162.
- [39] Potlog T., Duca D., Dobromir M., Temperature-dependent growth and XPS of Ag-doped ZnTe thin films deposited by close space sublimation method, *Appl. Surf. Sci.*, 2015, 352, 33-37.
- [40] Boufi S., Abid M., Bouattour S., Ferrara A.M., Conceição D.S., Ferreira L.F.V., et al., Cotton functionalized with nanostructured TiO<sub>2</sub>-Ag-AgBr layer for solar photocatalytic degradation of dyes and toxic organophosphates, *Int. J. Biol. Macromol.*, 2019, 128, 902-910.
- [41] Jradi K., Maury C., Daneault C., Contribution of TEMPO-oxidized cellulose gel in the formation of flower-like zinc oxide superstructures: characterization of the TOCgel/ZnO composite films, *Appl. Sci.*, 2015, 5, 1164-1183.
- [42] Deng Q., Duan X., Ng D.H.L., Tang H., Yang Y., Kong M., et al., Ag nanoparticle decorated nanoporous ZnO microrods and their enhanced photocatalytic activities, *ACS Appl. Mater. Inter.*, 2012, 4, 6030-6037.
- [43] Sung-Suh H.M., Choi J.R., Hah H.J., Koo S.M., Bae Y.C., Comparison of Ag deposition effects on the photocatalytic activity of nanoparticulate TiO<sub>2</sub> under visible and UV light irradiation, *J. Photoch. Photobio. A.*, 2004, 163, 37-44.
- [44] Zhao G., Kozuka H., Yoko T., Sol-gel preparation and photoelectrochemical properties of TiO<sub>2</sub> films containing Au and Ag metal particles, *Thin Solid Films*, 1996, 277, 147-154.
- [45] Jung H.J., Koutavarapu R., Lee S., Kim J.H., Choi H.C., Choi M.Y., Enhanced photocatalytic degradation of lindane using metal-semiconductor Zn@ZnO and ZnO/Ag nanostructures, *J. Environ. Sci.*, 2018, 74, 107-115.